IAC-20/C3/5-C4.10 BASELOAD FISSION REACTOR FOR LUNAR OPERATIONS

Peter J. Schubert, Jeel Doshi, Eli Munyala Kindomba, Adam Conaway, Amal Bhaskaran

Indiana University-Purdue University Indianapolis, Indianapolis, Indiana, U.S.A. pjschube@iupui.edu

Keywords: nuclear, fission, thorium, transmute, heat, power

ABSTRACT

Breakout performance for human operations will be realized once there are MW-class continuous-operation fission reactors on the Moon. This is likely to be realized only when there is a means for producing fissile fuel from ISRU resources, such as lunar thorium, because of the concerns associated with earth-launch of radioactive materials. Space is pervaded by gamma rays which produce neutrons upon interaction with beryllium. When moderated by graphite, said neutrons can be captured by the thorium nucleus, which transmutes into protactinium, which further decays into the U-233 isotope of uranium. U-233 is an excellent source because the radioactive byproducts of spent fuel are short-lived, becoming safe after about 80 years. Thorium dioxide (ThO_2 or thoria) is much more dense than the regolith average, and is found in concentrations exceeding those on earth in certain craters of the north Near Side, possibly because of the excavation of rich subsurface deposits due to meteorite impacts. Using jaw crushers and trommels made of durable lightweight metals a lunar mining operation can extract hundreds of kilograms of thoria by using a polymeric adaptation of a Wilfley sorting table laid along the sloped wall of a crater. An acid leach process can be used to remove intermediate protactinium from further neutron irradiation, which will decay to U-233. After processing, the transmuted urania (UO_2) is packed into fuel rods for a first-generation lunar fission reactor. The same gamma rays and beryllium will initiate a controlled chain reaction to provide baseload power. A Brayton cycle generator can produce power in a manner similar to the small modular reactor concept in development for terrestrial loads. With power outputs in the range of 1 to 60 MW, a single reactor can provide heat and power for a sizable human base plus mining operations, as well as electromagnetic launchers to deliver payloads into orbit. Water harvested from polar craters can be shipped to any orbit. Greenhouses on the Moon can become the breadbasket to the Solar System. Electric power can be delivered over transmission lines, or via wireless power transfer to a variety of loads such as rovers, orbiting spacecraft, and even multiple habitats. With no nuclear materials needing to be launched from the earth's surface, and with relatively short-lived hot waste, this is a pathway to the long duration settlement of the Moon.

INTRODUCTION

In January 1978 a nuclear reactor-powered satellite (Kosmos-954) crashed into northern Canada, spreading radioactive debris along a 600 km path. The massive clean-up effort was partly paid through the Space Liability Convention. Two similar satellites have plunged into international waters. Dozens more nuclear fission-powered satellites remain in earth orbit. Radioisotope thermal generators for long-duration, deep space missions draw power from radioactive decay of plutonium. While safer against rocket explosion than a fission reactor, concerned citizens stage angry protests whenever a manifest includes these toxic payloads. Terrestrial accidents such as Chernobyl, Three Mile Island, and Fukushima Dai-ichi understandably raise doubts and resistance to the prospect of launching 'nukes', regardless of how low the risk. An alternative is available using lunar resources.

The first atomic pile on the Moon may be similar to Chicago Pile-1 (December 1942) of the Manhattan Project which embedded uranium-containing briquettes in graphite blocks to produce a mild chain reaction capable of generating ample heat. Straightforward methods, described herein, can facilitate this simple nuclear reactor. A heat engine (Brayton or Stirling cycle) produces electric power. Such power can operate a lunar base, and enable in situ resource utilization (ISRU) to build a more sophisticated second-generation nuclear fission reactor (see paper IAC-20/C4/10-C3.5). The methods described herein of bootstrapping ISRU has the powerful advantage that it requires no radioactive material to be launched from earth.

METHODS

A. Fuel Materials Preparation:

Element 90, thorium, is about as abundant on the Moon as it is on Earth, with some areas having higher concentrations due to impact excavation of underlying strata in the lunar mantle. Measurements average 12 parts per million (ppm) with some areas likely at 20, and possibly a few at 60 ppm. Thorium is a fertile material, and can be transmuted into fissionable uranium via absorption of a thermal neutron and

a waiting period of one lunar day. The nuclear chemistry is described by this equation:

$$^{232}_{90}Th + n \rightarrow {}^{233}_{90}Th + \beta^- \rightarrow {}^{233}_{91}Pa + \beta^- \xrightarrow{27\ days} {}^{233}_{92}U$$

The sun is too far away to produce much of a neutron flux at the Earth's orbit. However, a convenient source can be generated by exposing the element beryllium (^{9}Be) to the high energy (> 0.1 MeV) gamma rays which pervade outer space from all directions. An intervening moderator of graphite is needed, which does not absorb neutrons, but provides recoiling nucleii that slow down fast neutrons until they are in thermal equilibrium with concentrated thorium, and can be captured. Thorium with a surplus neutron spontaneously emits a beta particle (electron), leaving behind an extra proton, and becoming the element protactinium. With a slower half life of 27 days, another neutron inside protactinium emits another beta particle and the atom transmutes again, becoming U-233. This is a fissionable isotope, similar in energy content to the enriched U-235 used in most terrestrial nuclear reactors, albeit with less-hazardous radioactive byproducts. The primary goal of this work describes how lunar thorium is beneficiated, transmuted, and packed into fuel rods for powering a first generation baseload lunar nuclear reactor.

Mining Rover:

The production process starts with the extraction of regolith and comminution to a particle size below 70 microns. To be able to extract the regolith, the design of the excavator was based on the rovers by Offword.ai with the addition of a front-end loader bucket. Each bucket-load of regolith is assumed to be 375 kg. Once at the production site, the bucket offloads excavated material onto belt feeders. The belt feeders deliver rock and dust to a gravity-independent jaw crusher.

Volume per scoop (m3)	0.25
Mass of the truck (kg)	500
Mass of the bucket (kg)	240
Density of regolith (kg/m3)	1500
Mass of regolith per bucket (kg)	375

Table 1: Rover Metrics

Using the above rover metrics, further calculations were conducted to get an approximate time taken to extract and transport 7000 metric tons of regolith. This is the quantity needed to obtain sufficient thorium for a stationary fission reactor of total power circa 6 MW.

Speed (m/s)	1.11
Average distance (m)	95
Travel time (s)	85.58559
Scoop time (s)	90
# of buckets	29166.67
Time taken to transport (s)	5121246
Time (years)	0.162373
Time (days)	59.27368

Table 2: Time required to transport regolith.

Jaw Crusher:

The jaw crusher uses hydraulic power to effect size reduction of the undifferentiated regolith. Cylindrical screens (trommel) are used to first remove fines which are already smaller than the target size, this being about half the mass of regolith. The jaw crusher progressively reduces the size of larger rocks until they meet the requirements of the downstream processing.

Commercial jaw crushers developed for terrestrial use are heavy and have higher throughput than are needed for lunar operations. To calculate power requirements and landed mass for a jaw crusher, a survey of available earth equipment was conducted to determine capacity versus mass. Figure 1 shows the lower end of offerings from four vendors, including a second-order least-squares fit curve which can be extrapolated to the relatively small processing rate needed. The intercept of this plot is 7.5384 MT (see equation), and for the capacity required of 2 MT/hour yields a jaw crusher mass of 7.54 MT.

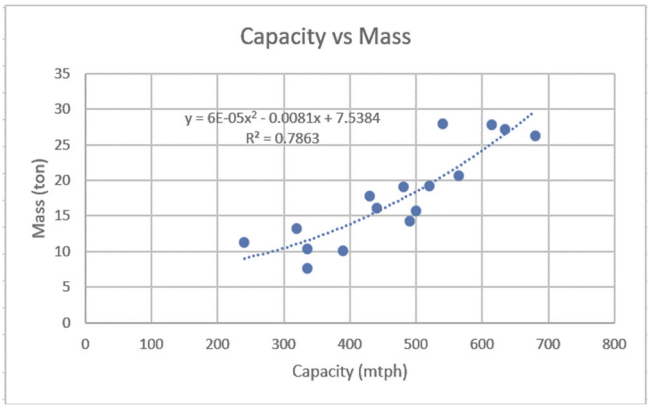

Figure 1: Jaw crusher scaling

Jaw Crusher Power Calculations:

With a scaled jaw crusher designed, it was crucial to understand the amount of power required to operate the machine. To calculate this von Rittinger's equation was used. Rittinger's theory states that the energy required for size reduction is directly proportional to the change in the surface area. (Rock Crushing Theory and Formula using Kick & Rittinger's Law, 2020):

$$E = K\left(\frac{1}{x_2} - \frac{1}{x_1}\right)$$

Where 'K' is the Rittinger's constant, x_1 and x_2 are the initial and final diameter of the particle, respectively.

To model the energy required to crush regolith, the value of K was taken as 62.5 kWh.µm/ton, derived from a study of crystallized sucrose being ground into powdered sugar. The density and final size for that application is similar to lunar regolith [Earle]. According to (Zolensky, et al.) for each 3x

increase in regolith particle diameter there is 30x reduction in the numerical density thereof. This factor was used to develop a particle size distribution function for computing the energy required to crush regolith using Rittinger's equation. To complete the 7000 MT within one earth year requires a steady power, during lunar daytime, of 17.85 kW.

Density Sorting Model and Calculations:

The next stage of production after the regolith is crushed to the desired size of 70 microns is to go through the density sorter. The purpose of the density sorter is to be able to separate target particles based on their density with the help of collision from a bullet particle (e.g. PTFE-coated ball bearings). Based on momentum transfer, when a bullet particle having lateral velocity impacts a target particle falling vertically in lunar gravity, lighter regolith particles are deflected more than those which are more dense. In this way, a relative concentration of the highly-dense thorium-bearing minerals can be effected. The yield per pass will be low, so the overall apparatus may be a cascade of such stages. This arrangement could advantageously be laid along the sloping sidewall of a crater or mountain on the moon. Such a density sorter may be considered a lunar adaptation of the time-honored Wilfley table used in terrestrial mining.

To determine the mass and the number of density sorting units needed the gravimetric feed rate was determined by:

$$Volumetric\ flow\ rate\ (\frac{m^3}{s}) \times\ density\ (\frac{kg}{m^3})$$

Then, the sorted fraction of regolith from one pass through the apparatus, compensating hit rate is found from:

$$Gravimetric\ flow\ rate\ (\frac{kg}{s})\ \times \%\ hit$$

Amount of thorium obtained by one pass in one apparatus:

$$Sorted\ Fraction \times ppm\ of\ the\ material\ (\frac{g}{kg})$$

The number of density sorting units to yield 15 kg of thorium from processing 7000 MT in one year is computed based on the duration of one pass. The mass of density sorting units to be delivered to the lunar surface is then computed by determination of the mass of each unit.

Using these specifications, it was determined that 61 density sorters will be required to be able to get 15,000 kg of Thorium, with the mass of each system being 241.87 kg, totaling 1.64 metric tons to process 7000 metric tons. Details of these calculations are presented in Table 3.

Depth (m)	3.50E-03
Density (kg/m3)	750
Width (m)	1
Height (m)	0.5
Mass of the apparatus (kg)	4
Drop time (s)	20
Hit rate (%)	0.5
# of runs to get desired conc.	50
ppm of U (g/kg)	0.0021
ppm of Th (g/kg)	0.012
Desired mass (g/year)	15000

Table 3: Specifications for the density sorter

A cross-sectional rendering of a density sorting unit is shown in Fig. 2. Bulk, comminuted regolith is introduced through a shaken hopper to fall vertically in lunar gravity. A hopper of the earth-made bullet particles ("shot") are also dropped to gain momentum, then diverted with a curved chute to impart a lateral velocity. The bullet particles pass through the cascade of bulk regolith. Each impact deflects regolith particles depending on their density.

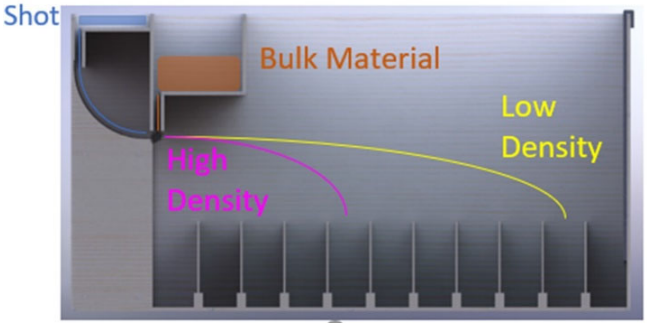

Figure 2 : Density sorter design (1 apparatus)

Fabrication techniques and sintering for pelletization:

After the regolith is crushed and sorted, it is ready to undergo fabrication and become pellets. There are a number of ways through which this can be achieved and based on the work of (Dasarathi et al. , 2013) some methods which seem viable, for the purpose of this study, is summarized in the table below.

PROCESS NAME	ADVANTAGES	DISADVANTAGES
Coated Agglomerate Process (CAP)	• Minimize dust • Few shielded operations • No binder • Low fission gas release	• Powder clean-up • Water recovery difficult
Impregnated Agglomeration Process (IAP)	• Limited powder handling • Homogeneous pellets • Easily shielded	• Needs binder (uranyl nitrate) mixed in • Requires earth re-supply
Sol-Gel Microsphere Pelletization Technique (SGMP)	• Dense, uniform pellets • Easily automated • No milling needed • Limited powder handling	• Complex, well-controlled process steps • Many speciality chemicals needed

Table 4: Fabrication method comparison

Modification of jaw crusher design for compaction:
Once the powdered regolith has been refined through the density sorter and fabricated, it needs to be compacted into pellets. To cut down on shipping mass as well as the extra labor to install another system, a novel design idea was proposed. Once the jaw crushers complete their job of crushing regolith, a special component added within the jaws allows the same apparatus serve as a mechanism for compacting the transmuted uranium oxide (urania) powder to make pellets. This arangement is shown in Fig. 3.

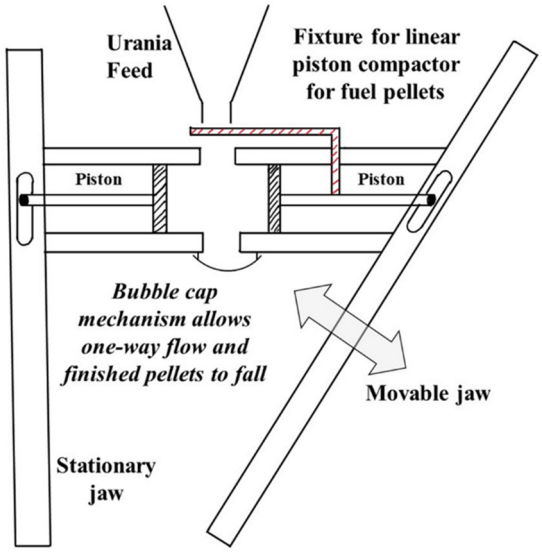

Figure 3: Proposed sketch of modified jaw crusher with compaction mechanism installed.

This new design helps save shipping extra mass from the Earth and thus save costs. However, the addition within the design of the jaw crusher leads to more customization of the machinery and requires the presence of an operations personnel on the lunar surface to install the system. A full time equivalent (FTE) staff of four is anticipated to install, operate and move material through this stage of operations.

B. Transmutation, Reactor Design & Siting

The first reactor will be based on early models of reactors developed on Earth. Due to the limits on production and assembly in the early stages, fuel rod composition and placement will be kept simple. With the exception of the uranium fuel, all the reactor components will be assembled on Earth. This includes the reactor core, steel shell, steel helium pipes, graphite moderators, control rods, beryllium reflectors, and all other necessary components. Special attention is given to the introduction of fuel rods, comprised of long metal pipes packed with many individual fuel pellets. These are to be inserted, and activated, only when the apparatus is assembled on the Moon.

Total potential power was calculated using the energy density equation. Operation time was calculated based on a goal of 2 MWe electrical energy and a 30% efficiency converting thermal energy to electric power. The size and design of the helium pipes was calculated based on the helium mass flow rate assuming a closed-loop Brayton cycle power system.

1. Components:

The reactor design is a cylinder having a lateral long axis and a radial arrangement of heat pipes. Control rods are raised and lowered from the top. The stainless steel shell is supported by short brackets which will rest upon the lunar bedrock. The design in figure 4 was used to estimate the mass and placement of the fuel rods, control rods, moderator, thermodynamic piping, reflector, and shell,

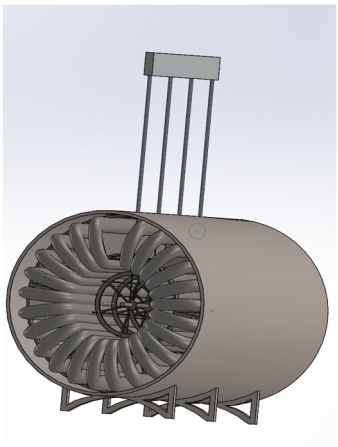

Figure 4: Simple Reactor Structure

1.1 Fuel Rods:
Our mass of UO_2 for the first generation reactor will be 28 kg with roughly 15kg being U-233. The shape of the fuel pellets will be cylindrical with a diameter of 1.5 cm and a height of 1 cm (Yacout). The rods will be placed into a steel or zircalloy casing, and separated by graphite cylinders. Graphite disks of 2mm height will also be inserted in the fuel rods between adjacent fuel pellets. Fuel pellet density should be approximately 10.6 g/cm^3 (Afifi). Placement of fuel rods was not calculated, but assumed to be appropriate for heat generation and proper control.

1.2 Control Rods and Moderator:
For safety concerns, boron carbide will be used for the control rods instead of cadmium. The rods will be inserted into the reactor at an angle perpendicular to the fuel rods (see figure 4) and will be controlled from the surface either by automation or by suitably-protected workers.

1.3 Piping for Thermodynamic Fluid:
Our thermodynamic fluid will travel through our reactor by stainless steel piping. Stainless steel 304 has a specific density of 7.85 Mg/m^3 (Azom.com). Length and diameter of our

piping were calculated based on the mass flow and volume flow rates of our thermodynamic fluid. A nominal thickness was assumed, though subject to change upon further thermal conductivity evaluation. Numbers were calculated for both helium and carbon dioxide as the working fluid.

1.4 Core Shell and Reflector:

Our shell and structural components will also be made of stainless steel with a beryllium coating as the neutron reflective material. The coating of the beryllium will be at an appropriate thickness so as to minimize neutron loss. Note that the exposure of this beryllium coating to cosmic gamma rays, in regions not having a moderator, will generate the hot neutrons required to initiate the controlled chain reaction.

2. Thermodynamic Working Fluid:

Possible choices for the thermodynamic fluid includes helium, helium compounds, or carbon dioxide. Densitities for the fluids were taken from engineeringtoolbox.com. The fluid will have to absorb 6MW of power from the core. Mass flow and volume flow can be calculated from a balanced energy equation.

$$o = \dot{Q}_{cv} - \dot{W}_{cv} + \dot{m}\left[(h - h_o) + \frac{(V^2 - (o)^2)}{2} + g(z - o)\right] \quad (8)$$

From the above equation, energy due to work, gravity, and velocity are eliminated. The calculations assume a pressure of 10 bar and a gas velocity of 10m/s.

Properties	Helium	Carbon Dioxide
Specific Heat (kJ/kg*K)	5.19	0.846 Inlet 1.075 Outlet
Density (kg/m^3)	1.744 Inlet 0.829 Outlet	20.88 Inlet 9.22 Outlet

Table 5: Properties of helium and carbon dioxide

It is unlikely our reactor will operate above a temperature of 573K, so an assumed inlet temperature of 273K and an assumed outlet temperature of 573K was used.

Placement of the reactor was based on proximity to resources, terrain, and radiation control. According to "Managing Space Radiation Risk in the New Era of Space Exploration," a reactor placed on the surface would require a distance of 1km from settlements. However,

- Evaluate whether to make a true fission reactor, or a "pile" reactor akin to the first atomic pile at Univ. of Chicago in 1942. All we need is heat to make electricity.
- Design site to be as near as possible (to keep transmission losses/mass low, but far enough to reduce negative impact)

C. Power and Heat Management

1. Brayton cycle conversion system

The proposed power production system will utilize a Closed Brayton Cycle (CBC) conversion system which offers a low mass, highly scalable (kilowatts to megawatts) power generation option to support various architectures (Mason et al., 2002). The basic components of a Brayton Cycle converter are a turbine, compressor, alternator (generator) and the waste heat rejection. Additional components can include separate heat exchangers for the heat source and the waste heat rejection and a recuperator. In a CBC, the working fluid (typically an inert gas), is heated by the reactor and supplied to the CBC to drive the turbomachinery, mounted with the electrical generator on a single or multiple shafts.

According to Juhasz (2007), design drivers for lunar power systems consist of:

- Minimum system mass
- High reliability, long operational life, little maintenance
- Few complex systems with minimum components.
- Trade between thermal efficiency in order to obtain low mass by removing several components (such as heat exchangers and regenerator).

Considering all these aspects, the purpose of the present section is to investigate the main power generation components requirements (turbine, compressor, generator), the working fluid, and the system configuration.

1.1. Working fluid

Working fluids heavily influence the size, geometry and performance of the Closed Brayton Cycle. Several working fluids have been proposed to be used with a Closed Brayton Cycle (Tournier and El-Genk, 2008). Three parameters, namely the pressure losses, heat transfer coefficient, and the aerodynamic loading, were calculated and compared in the selection of a working fluid.

In this study, using correlations developed by Tournier and El-Genk, a comparative analysis is performed to predict the thermodynamics properties and previously listed parameters of several working fluids, namely Helium, He-Xe (15 g/mol, 8.6 mole% Xe & 91.4 mole% He), He-Xe (40 g/mol, 28 mole% Xe & 72 mole% He), He-N_2, N_2, H_2O, H_2, CO_2 and O_2.

The equation for the turbulent flow heat transfer coefficient for gases rearranged by Tournier and El Genk (2008) can be expressed as:

$$h=0.023(T_w/T_b)^{-c}\times\dot{N}^{0.8}\times[D^{-0.2}\times A^{-0.8}]\times[(M^{0.8}k^{0.35}c_p{}^{0.15})/\mu^{0.15}] \quad (9)$$

When only considering variables representing Gas properties and keeping operational and geometrical variables constant in equation (9), the relative heat transfer coefficient is given as:

$$h_{RT}=h/h_{He} \propto (M^{0.8}k^{0.35}c_p^{0.65})/\mu^{0.15} \quad (10)$$

Selection of a working fluid with high heat transfer coefficient will impact the heat transfer surface areas and hence, the size and mass of the radiator gas cooler and recuperator (Tournier and El Genk, 2008). Therefore, the higher the heat transfer coefficient, the lower the size of the radiator gas cooler and recuperator.

According to Tournier and El Genk (2008), the relative pressure losses can be solely expressed in terms of gas properties as shown:

$$(\Delta P/P) \propto (\mu^{0.2}M^{0.8}Z) \quad (11)$$

As for the aerodynamic loading, this parameter can be indicated by the enthalpy rise in the compressor as shown below

$$\Delta H_c = (\widehat{C}_p/M)T_{1,o}\,[\pi^{(\gamma-1)/(\gamma\eta_c)} - 1] \quad (12)$$

As explained by Tournier and El Genk (2008), the size of the turbomachinery depends on the magnitude of the aerodynamic loading, indicated by the enthalpy rise in the compressor. Results from Tournier and El-Genk's calculations clearly showed that the molecular weight of the working fluid (in their case, a binary mixture) is inversely proportional to the loading in the compressor and hence, the size and mass of the turbomachinery.

The reference temperature and pressure conditions used for calculations are 400 - 1200 ºK and 0.1 - 2.0 MPa for CBC conversion loops. Working fluid thermophysical properties were drawn from the NIST database (Lemmon, 2020).

1.2. Turbomachinery

Due to the extensive amount of test data available for axial compressors and turbines using air as a working fluid, it was decided that the turbomachinery will utilizes multi-stage axial compressor and turbine technology adapted from stationary power plants but modified for appropriate CBC working fluid. (LaFleur, 1963). Technology development for multi stage axial/radial compressor and turbine technology can be applied in this case. For this study, high-strength nickel alloys can be chosen as turbine and rotor material for temperature levels up to 2000 R or 837.9 C (Kofskey and Glassman, 1964). Selected material for pipes is stainless steel for temperatures beyond 300 C (Linares et al, 2016).

The individual masses for key sub-systems (Turbine, compressor, generator) were determined by use of empirical mass models and estimates based on a survey of current gas turbine technologies. According to Christopher (2020), turbomachinery components (compressor, turbine and alternator) have low specific masses and scale based on power requirements. Christopher notes that in general the turbomachinery mass is not dominant in the mass budget, though it is dominant in the technology development piece (Christopher , 2020).

Christopher (2020) based turbomachinery models on trendline from Juhasz (Juhasz, 2005) and used the equation below to obtain a model-based mass of the turboset.

$$m_{turboset} = 933P_e^{0.7}\,(1 + 0.53\ln(PR)) \quad (13)$$

In this equation, PR represents the compressor pressure ratio, Pe the electric power of the alternator (generator) in MW and the turboset mass is in kilograms. Christopher (2020) points out that the equation above is most applicable to the 1100 to 1300 ºK temperature range (turbine inlet hot temperature) and is only a first-order approximation for systems outside that range.

In this analysis, electric power is fixed at 2 MWe. Compressor pressure ratio is varied from 1.5 to 3.5. Technology developments for compressor and turbine polytropic efficiencies above 85% have been demonstrated and alternator efficiency can typically reach 95% (Christopher, 2020). In addition, it has been shown that turbomachinery components scale strongly with power. At MW-power levels, turboet specific mass gets close to 1 kg/kWe and goes below 1 as the power increases beyond 5 MW (Christopher, 2020).

One issue on the moon will be meteoroid protection. In order to protect the turbomachinery cover structure from meteorite impact, micrometeoroid and orbital debris (MMOD) shield configurations, similar to the ones developed by NASA and the ESA to protect the U.S. Laboratory Module and the European pressurized laboratory Columbus, are proposed to be used in order to provide adequate protection (Cherniaev, 2016).

For working fluid pipe materials, the amount of shielding needed depends on the environment, reliability requirements, exposed area and time. On the lunar surface, the meteoroid environment is less than encountered in orbit/space away from the moon, because of the shadowing/shielding provided by the moon itself. However, there is a secondary ejecta environment that needs to be considered for the lunar surface that is not present for spacecraft in orbit away from the moon (Christiansen, 2020).

To shield the fluid pipes, a flexible fabric/foam wrap, glass fabric on the outside, Kevlar near the pipe, and foam between them, about 5 cm thick, around the pipe would probably be sufficient provide adequate protection for a service life of at least 6 years (Christiansen, 2015, 2020).

1.3. System configuration

As shown in figure 5 below the system configuration consists of a single gas-cooled reactor that heats the working fluid and that is directly coupled to one Closed Brayton Cycle (CBC) loop. A large radiator panel system removes the heat in the outer space heat sink. The proposed CBC does not include heat exchangers nor regenerators which increase the overall system mass, cost and lower reliability. This trade-off will lead to a lower efficiency (Juhasz, 2006).

Removal of usually large recuperative/regenerative heat exchangers reduce the overall thermal efficiency for the sake of providing low mass and higher reliability (Juhasz, 2006). In one case, Juhasz described an efficiency value of 10 percent lower than what could have been obtained with regenerative heat exchangers but a launch mass gain of at least 6 metric tons.

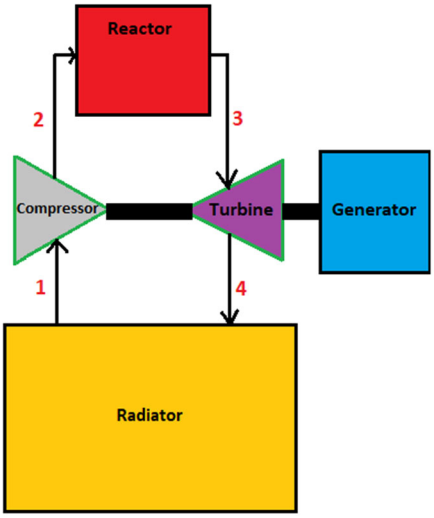

Figure 5: Simplified schematic of lunar CBC power plant

Table 6**:** Station location for temperatures and pressure at various locations

Station Number	**Inlet Component**	**Outlet component**
1	Compressor inlet	Radiator outlet
2	Reactor inlet	Compressor outlet
3	Turbine inlet	Reactor outlet
4	Radiator inlet	Turbine outlet

2. Lunar Surface-to-Surface Power Transfer

The multiple surface elements and payloads will each require electric power. One requirement for the moonbase powerstation is to transfer electric power up to 2 MWe across the lunar surface to distances as low as 100 m to support human habitats and ISRU production plants. Several state-of-the art power transfer subsystems including AC or DC power cables, beamed radio frequency and beamed laser have been investigated based on quantitative and qualitative metrics. DC power cable was selected as the simplest and most mature technology with lower mass, lower component count, lower source power, higher power transfer efficiency, less technology development need and long-term operation without maintenance and risk (Kerslake, 2008).

The reported performance analyses of the MW lunar power transfer systems have solely been based on simplified models and extrapolations of previous assessment study done by Kerslake. Kerslake developed spreadsheets-based tools for power levels between 1 to 50 kW and transfer distances between 0.1 km to 10 km. Quantitative metrics included power transfer subsystem mass, power source plus power transfer subsystem mass, input power to output power, power transfer subsystem efficiency, net payload element power (Kerslake, 2008).

DC Power Cable Concept Design Inputs and Assumptions

The goal of the subsequent analysis is to demonstrate scalability of DC power transfer from kW to MW levels. The DC power cable is set to transfer source electric power of 2 MWe with flat-rested cable of length 100 m to nearby payloads. Starting reference inputs for source voltage was set at 160-VDC with source power from 1 to 50 kW and other assumptions are shown in table 7 below.

Table 7: Reference DC power cable inputs and assumptions

Source voltage	160-VDC
Source Power Input	1 to 50 kW
Cable power efficiency	0.75 to 0.997
Wire size	AWG size of 16 or less
Cable temperature	300 K
Cable length	0.1 to 10 km
Cable connectors mass	1 percent cable mass fraction
Control cabling mass	0.05 kg/m
Active thermal control system (ATCS) mass	6 kg/m^2 radiator area
Data/control cable mass	5 percent cable mass fraction

Deployment	Spool-deployed
Material	Copper
Electronics control temp.	353 K
Cable output voltage	1000 VDC
Secondary structures mass	5 percent system mass fraction
Spool and Deployment mechanism mass	50 kg

Power electronics mass and performance calculated by Kerslake illustrated the dependence of payload power level with a fixed 1 km cable length as shown in figure 6 below. It was determined that at a fixed distance, DC power cable system mass increases proportionally to the payload power, and in the same token, proportionally to the source electric power.

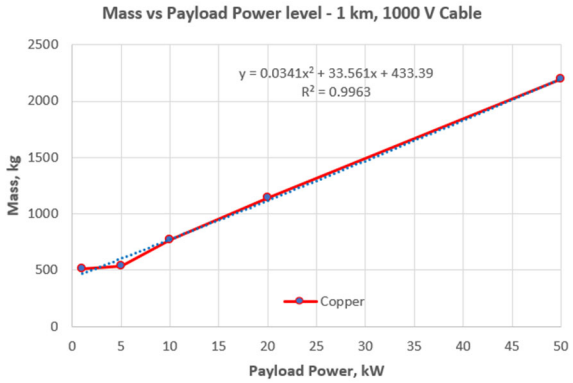

Figure 6: Mass vs Payload power at fixed 1 km length

Spreadsheets models developed by Kerslake also illustrated the dependence of the source power on cable length. At fixed payload power of 10 kW, the source power increases with increasing cable length (fig. 7).

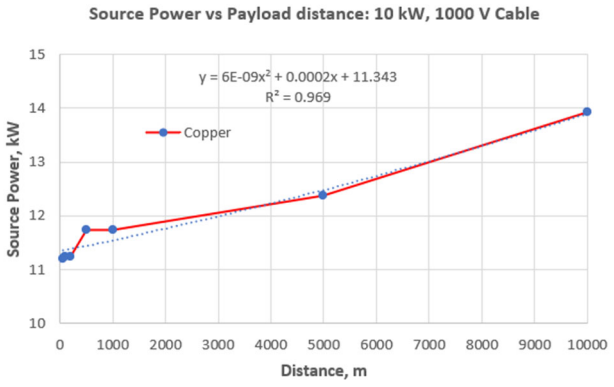

Figure 7**:** Source Power vs payload distance at fixed 10 kW

Using the reference input data in figs. 6 and 7, trendlines (curve fits) are used to extrapolate mass data for power levels up to 2 MW at cable length of 100 m.

D. Operational Safety and Performance Metrics

Reactor Safety : The initial stages of setting up the lunar base to mine thorium and generate energy through the reactors involves the mining process. It is during this initial mining of lunar regolith that the foundations for the remaining base will be set up, this includes excavating a whole twice the depth of the reactor and the same radius or length of the reactor to create a safe area to place the nuclear reactor in. The purpose of this is to provide a safe and effective safety system in the case of reactor meltdown. The inner walls of the reactor bin will be coated by the preferred material that can be obtained from lunar regolith for better shielding.

Reactor Performance: The heat dissipation of the reactor is reliant on the radiation panel arrays, these arrays even though effective at dissipating heat during lunar night time conditions do not effectively dissipate heat during the day, a workaround solution must be brought into ensure proper heat dissipation around the clock. Reactor maintenance requires sophistication and timely reactions from the operators point to ensure that the system runs at maximum efficiency, as this is a difficult task for rovers and robots to perform and the effectiveness of using such automated maintenance systems must be measured. There must also be strict protocols on the maintenance of the reactor along with the disposal of nuclear waste.

As there is a possibility for human operators to be present, the other aspects of the operation must also be analyzed to ensure whether humans or robots are effective. And as such a Full Time Equivalent (FTE) workforce must be calculated to understand the requirements of humans, this can be done by measuring the amount of time to do a particular task in one week and dividing that number by 40 to obtain the FTE.

RESULTS

A.Fuel Materials Preparation

<u>Power calculations and mass needed for solar energy:</u>
The production system is the first phase in the overall project and hence when installed there will be no source of power available to conduct operations. Due to the lack of atmosphere on the lunar surface, there is a high amount of solar irradiance. This results in a great opportunity to utilize this free source of energy and implement solar panels to power the initial stages of operations. To estimate the amount of mass and area required to install for solar panels, the amount of power needed to operate the production system was compiled. Using a specific power of 20W/kg for

the solar panels, the total mass was determined. To calculate the area, the following equation was used:

$$Total\ power\ (W) = Total\ area \times solar\ irradiance \times conversion\ efficiency \quad (14)$$

Power to lift (W)	10.7625
Jaw Crusher + Compaction Power (W)	3.57E+04
Belt Feeder (W)	416.1
Screener (W)	1.50E+04
Approximation for fabrication (W)	2.00E+04
Total Power Required (W)	71126.8625

Table 8: Total Power for production

Based on the total power calculated as shown above in Table 8, the total mass of solar panels needed is 3556 kg, with an area of 145.70 square meters.

Total shipping mass:
A summary of the various components that will need to be shipped from the Earth to set up production is shown in the table below.

	Mass (kg)
Solar Panels	3556.343
Jaw Crusher	7.50E+03
Density sorter	1.64E+03
Rover (x4)	2960
Screener	250
Belt Feeder (x4)	2.00E+03
Fabrication system	2.50E+03
Sintering furnace	200
Total	20606.34

Table 9: Total mass for production.

An approximate 21 metric tons of equipment will need to be shipped from the Earth to establish the production system. Four rovers will be shipped, with two rovers working during production time, while the other rovers remain as a standby and in case of emergency vehicles. Four belt feeders will be needed to ensure smooth connections between the different stages in the production plant and to allow for a continuous feed rate into the system.

Selection of fabrication method:
From Table 4 various benefits and disadvantages were summarized about some viable fabrication options. On evaluating these methods, the CAP method seems to be the most appropriate. Except for the addition of water the CAP does not require the addition of any external liquid binders and with the system only requiring to be partially shielded, it simplifies the installation of the system. To address the issue with the addition and the recovery of water, a simple condensation chamber can help retrieve and recycle the water. This helps in reducing the dependence of receiving more resources from Earth.

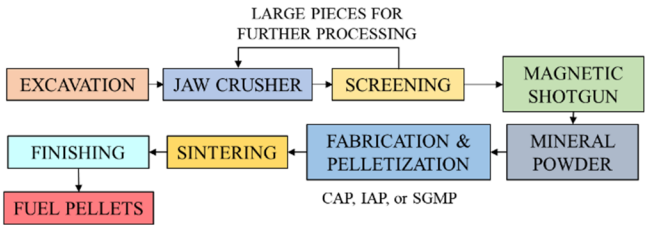

Figure 8: Proposed Production process.

The above figure shows the proposed flow chart from excavation to getting the result of pellets. The processes will be connected with the help of belt feeders, and collection will be in bins. These bins will be transported with the help of rovers. The entire process, except sintering, will have to be conducted in a shielded facility, to avoid particles from straying away and to allow for controlled production. Other than the required measures that need to be taken for fabrication, such as with the CAP method, no other special shielding is required. Sintering will be carried outside, since the heat energy will primarily come from concentrated sunlight. Along with this, having the sintering furnace outside the shielded production facility also acts as a safety precaution, in the event of a mishap, other equipment will be safe with minimum to no damage.

B. Transmutation, Reactor Design & Siting

The goal for total thermal power generation is 6 MW. From the energy density equation, 15 kg of uranium will provide 5.92 years of energy at the maximum. As fuel is used up, the total power output will eventually begin to decrease. By the time the reactor is no longer functional, more advanced reactors will be utilized. The first generation reactor will be used to power mining and processing equipment and living quarters for workers.

1. Internal Core Design

The first-generation reactor will be a small reactor, thus only 12 fuel rods will be used, arranged in a hexagonal formation around the fluid piping. Each rod will be composed of 187 fuel pellets. With the carbon spacers, this gives an overall fuel rod length of 317.9 cm. Four rods of born carbide will be used as the control rods, each with a length of 1.8 m. The rods will be attached to steel rods that run to the surface to allow for adjustments.

2. Helium

From the properties of helium and a balanced energy equation, the mass flow rate of the helium will need to be 3.85 kg/s. At the inlet this is a volumetric flow rate of 2.21 m^3/s and at the outlet this is a volumetric flow rate 4.65 m^3/s. From

a design utilizing 24 flow pipes, this leads to an inlet radius of 5.4 cm and an outlet radius of 7.85 cm.

3. Carbon Dioxide

We can use the properties of carbon dioxide to calculate our inlet and outlet pipe data. The inlet mass flow rate will be 23.64 kg/s and the outlet mass flow rate will be 18.6 kg/s. Using the respective densities and assume 24 pipes, this gives and inlet pipe radius or 0.5 cm and an outlet radius of 0.7 cm.

4. Placement Design

Given the high velocity of our fluid, and the large amount of energy transfer, it was important to use return piping. Both inlet and exits will be on the same side of the reactor. Total piping length will be 10m.

Helium is our preferred fluid given its high specific heat and relative stability across inlet and outlet. However, given its low density, large diameter pipes will be required. To allow for the piping, the minimum diameter of our reactor is 244 cm. This also allows plenty of space for the nuclear fuel, control rods, and moderators.

C. Power and Heat Management

1. Closed Brayton Cycle

Working Fluid

Results of calculations for the working fluid parameters are highlighted in the current sections. Comparative analysis of normalized heat transfer coefficients, pressure losses and aerodynamic (compressor) loadings, using helium as the reference metric, are displayed below.

At typical operating conditions in space reactor power systems with CBC conversion loops of 0.1 - 2 Mpa and 400 K - 1200 K, He-Xe (40 g/mol) has the highest pressure losses, 6 times higher than He as shown in figure 9 below.

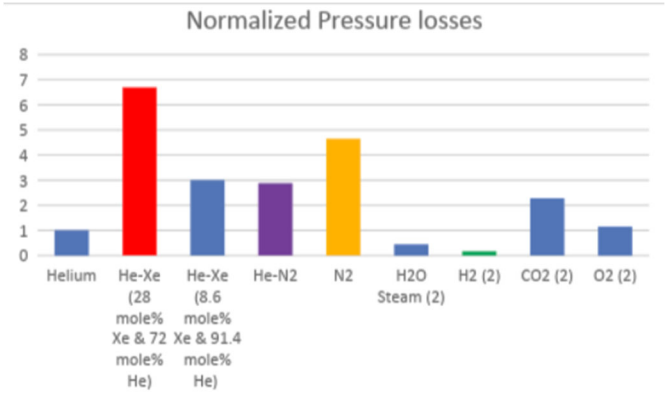

Figure 9: Normalized pressure losses

A summary of the pressure losses conclusions is displayed in table 10 below. It can be seen that hydrogen gas (H_2) has the lowest pressure losses, about 16% that of helium, which is a widely cited working fluid.

Table 10: pressure losses compared to He.

He	Standard
He-Xe (40)	6 times more pressures losses than He
He-Xe (15)	3 times more pressures losses than He
He-N2	2.8 times mores pressures losses than He
N2	4.6 times more pressure losses than He
H2O	Only 44% of He pressure losses
H2	Only 16% of He pressure losses
CO2	2.27 times more pressure losses than He
O2	1.14 times more pressure losses than He

Comparative analysis of values of normalized heat transfer coefficients is shown in fig. 10 below. According to Tournier and El-Genk (2008), Helium has the highest heat transfer coefficient of all noble gases. However, binary mixtures of He with other gases have slightly higher heat transfer coefficients. He-Xe (15 g/mol) has the highest heat transfer coefficient of all the noble gas mixtures.

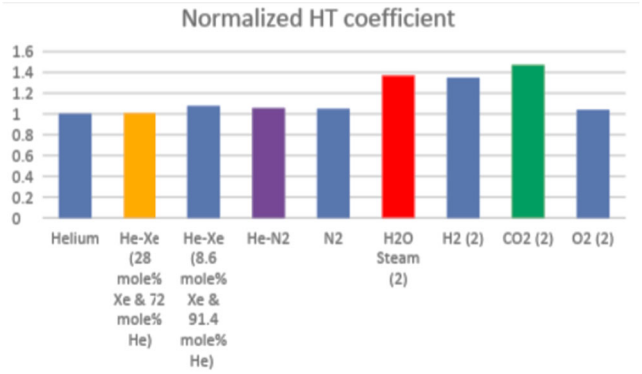

Figure 10**:** Normalized Heat transfer coefficient

From this analysis, CO_2, water and H_2 have the three highest heat transfer coefficients.

As for the compressor loading comparison (fig. 11 below), He-Xe (40 g/mol) has the lowest aerodynamic loading, followed by nitrogen. CO_2, which is an attractive working fluid, has an aerodynamic loading of 31 to 38 % of the loading of He. Table 11 below summarizes the comparison of each working fluid with He.

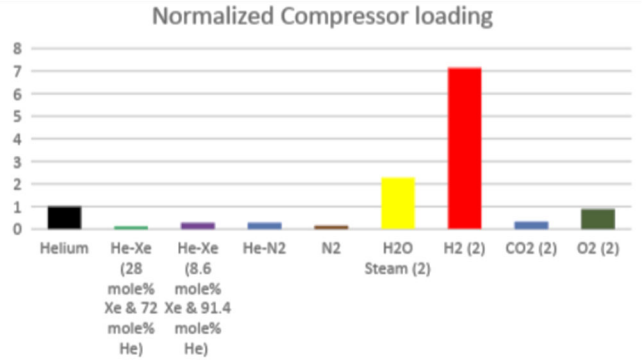

Figure 11: Normalized compressor loading

Table 11: Normalized compressor loading compared to He

He	Standard
He-Xe (40)	Only 10% of He aerodynamic loading
He-Xe (15)	Only 26.7% of He aerodynamic loading
He-N2	Only 26.9% of He aerodynamic loading
N2	Only 13.7% of He aerodynamic loading
H2O	2.275 times more aerodynamic loading than He
H2	7 times more aerodynamic loading than He
CO2	Only 31-38% of He aerodynamic loading
O2	Only 87% of He aerodynamic loading

In summary, Helium has the best transport properties of noble gases and robust heritage in test plant and design studies (Olumayegun, et al., 2016). Although He binary mixtures such as He-Xe (40 g/mol and 15 g/mol) have attractive transport properties and low aerodynamic loading, they have 3 to 6 times more pressure losses than He.

In this analysis, nitrogen demonstrated acceptable transport properties with low aerodynamic loading. In addition, Nitrogen is commercially available. However, high pressure losses, the likelihood of nitriding and of embrittlement of material at high temperatures play to its disadvantages (Olumayegun, et al., 2016). Supercritical CO_2 has demonstrated good transport properties at moderate to high temperatures and low aerodynamic loading compared to He. However, disadvantages of CO_2 as a working fluid include high pressure losses, corrosion issues as temperature increases, limited design experience, likelihood of operation and design challenges due to rapidly varying property near the critical point of 7.3773 Mpa, 30.978 C (Olumayegun, et al., 2016).

For the first generation CBC plant, Helium seems to be the working fluid of choice. As previously mentioned, helium has a robust though limited design and testing experience, low pressure losses, good transfer properties. In addition, as a noble gas, helium remains inert and non-toxic. Disadvantages of helium include high leakage and high number of compressor stages which means bigger mass and size the compressor (Malik, et. al, 2020). Due to its small atomic radius, helium can leak through most materials used to contain it. Flessas (2020) proposed the use of adhesive sealants to help prevent leakage. In addition, Flessas adds that compressors designed for helium applications are doubly sealed, in addition to using specialized safety valves at each compression stage.

Turbomachinery

The mass estimates, based on trendline models and the correlation expressed by equation (13) are shown in table 12 below. For payload electric power of 2 MWe, mass estimates for the turbomachinery are between 1800 and 2550 kg. Christopher (2020) suggested the use of a two-times mass factor based on three model limitations:

- missing structural mass, pipes and connections between components in the model;
- neglect of turbine windage, compressor bleed and electromagnetic losses
- large uncertainty in all components partially based on empirical models and simple designs.

Table 12**:** Turbomachinery mass estimates as a function of compressor pressure ratio.

Power (MWe)	PR	Turboset Mass (kg)	Specific Mass, kg/kWe	2x Mass Factor
2	1.5	1841.37365	0.920686825	3682.747301
2	1.8	1987.832808	0.993916404	3975.665615
2	1.9	2031.265081	1.01563254	4062.530162
2	2	2072.469055	1.036234527	4144.93811
2	2.5	2251.720576	1.125860288	4503.441153
2	2.8	2342.757665	1.171378833	4685.51533
2	3	2398.179734	1.199089867	4796.359467
2	3.2	2450.023616	1.225011808	4900.047233
2	3.5	2522.009187	1.261004593	5044.018373

A separate survey of turbomachinery technologies available for gas and steam turbines and aircraft on earth can be used and adapted to Helium working fluid. Tables 13, 14, and 15 below summarize turbomachinery technologies that can be adapted to the moon base power conversion system.

Table 13**:** Commercial turbine technology portfolio.

Turbine	Manufacturer	Output power	Mass (kg)
ASE40	Vericor [28]	3.2 MW	601
ASE50B	Vericor [28]	3.682 MW	654
Saturn 20	Solar Turbines [29]	1.185 MW	6805

Table 14: Commercial compressor technology portfolio

Compressor	Manufacturer	Mass (kg)	Max Speed (RPM)
C16	Solar Turbines [29]	1996 - 2540	23,800
WP6550	Sauer Compressors [30]	3991.6	1780
WP316L	Sauer Compressors [30]	1122.64	1770

Table 15: Commercial generators technology portfolio

Generator	Manufacturer	Mass (tn)	Max Speed (RPM)	Power rating (kVA)
ECO 46	Mecc Alte [32]	3-5.12	1500/1800	1300 - 2500
PMG2200	The Switch [31]	5.6	1500	2200
AMG 500	ABB [33]	5 - 7	1800 rpm	1.5 - 3.6 MW

2. Power transfer performances

At the same power condition (10 kW) and voltage rating (1000V), and using data used to obtain fig. 7, it is shown that total power cable system mass increases with increasing payload distance or cable length (see fig. 12 below).

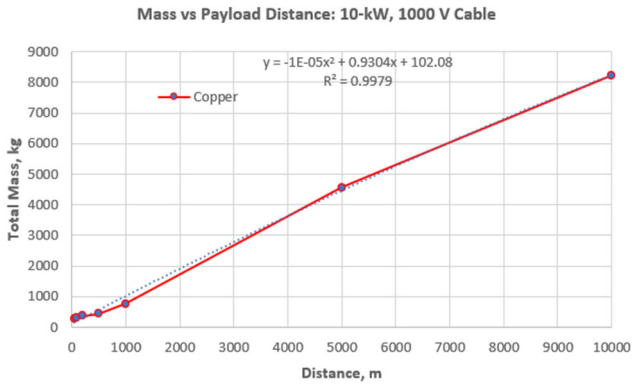

Figure 12**:** Mass vs Payload distance at fixed 10 kW

Using the 2nd degree curve fit equation in fig. 6**,** the total mass of the system at 2 MW payload power is beyond 200 metric tonnes at a distance of 1000 m (reference distance). However, from fig. 12, cable power transfer system specific masses at 10 kW for 100 m and 1000 m are 29.36 kg/kW and 76.65 kg/kW respectively. The specific mass ratio from 100 to 1000 m is 0.38.

Using fig. 6, it can be demonstrated that the cable system specific mass at a fixed cable length decreases with increasing payload power. Thus, using reference data from fig. 6, a graph of system specific mass vs payload power at 10 kW is obtained as shown in fig. 13 below.

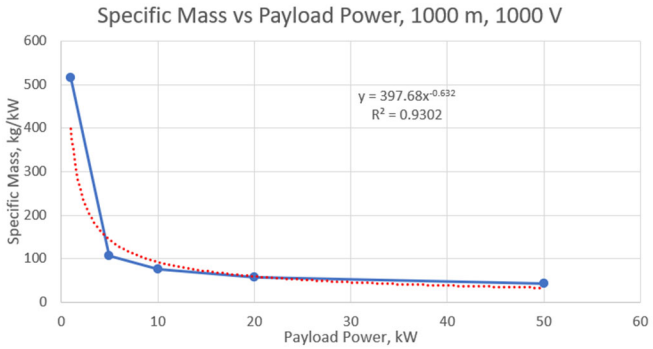

Figure 13: Specific Mass vs Payload power at fixed 1 km

In the case illustrated by fig. 13, the extrapolation uses a power fit. Using that best-fit equation, a payload power of 2 MW will have a specific mass of 3.26 kg/kW at 1000 m. Multiplying this value by the specific mass ratio of 0.38304, the cable system specific mass for 2 MW at 100 m is 1.249 kg/kW. This value of specific mass is consistent with MW level projects such as the European Union's MEGAHIT project which places the specific mass of the power management and distribution system under 1 kg/kW (Christopher, 2020). Key outputs for the DC power transfer cable system are shown in table 16 below.

Table 16: Key DC power cable system output parameters

Payload Power	2 MW
Cable length	100 m
Cable System specific mass	1.249 kg/kW
Total DC Cable system mass	2497.79 kg

Concept of Operations

The DC power cables will be flat rested on the lunar surface. Kerslake proposed to have the source power electronics and power cable assembly pre-integrated with the moon base powerstation (Kerslake, 2008). A mechanism to straighten the cable will be needed in order to reduce free coiling. Cables on the payload side will be deployed and installed on a rover that will pull them to the source power and dock power and data connectors.. Appropriate verification procedures will be

executed before allowing power flow). A flexible fabric/foam wrap, similar to the one used on pipes will be used for meteoroid armoring.

Heat Rejection

The thermodynamic fluid will be brought from the turbomachinery and put through Carbon composite material. The design of the radiators as shown in figure 14 is a base of heat pipes that indent into the carbon composite layer on the top of the radiator panel. Each panel is 2 meters wide and 0.15 meters thick including the C-C film of 0.01601 meters. To provide complete dissipation of heat 11 of 60 meter long panels must be placed within a 2 meter deep trench.

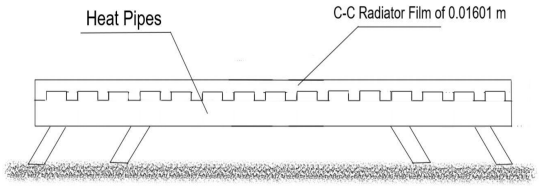

Figure 14. Radiator Side profile

1. Powerstation layout

Location

Investigation of suitable powerstation locations led to the establishment of four main requirements:

- Proximity to thorium-rich craters and lunar volcanic material
- Relatively level topography for landing, operation base, and rover operations.

Thorium on the lunar surface has been located in high concentrations around the Imbrium basin region and near Aristillus crater, Aristarchus crater, Mairan crater, Kepler crater, the Fra Mauro region near the Apollo 14 landing site, the Apennine bench region near the Apollo 15 landing site, and the highlands regions north and northwest of Imbrium basin (Lawrence et al., 2000). Those thorium-rich regions, which tend to display central peaks, terraces, and flat floors (such as Kepler crater with a diameter of 32 km), will be suitable for the thorium extraction and processing and lunar power station location.

CBC Layout

The turbine, compressor and generator will be connected by a single shaft and oriented horizontally. This horizontal layout provides ease of maintenance and reduces possibility of bearing failures (Olumayegun et al., 2016). Similar to the GT-MHR facility designed in the 90s, the CBC power conversion system will be enclosed in a structural vessel, likely made of hardened aluminum. The turbo-machinery will be placed above ground to reduce the need for further excavation and for ease of access.

Shielding

Shielding requirements for turbomachinery structure include the use of an all-aluminum Whipple Shield (WS) to provide protection against millimeter-size particles (Cherniaev and Telichev, 2016). Areal density parameters for that Whipple Shield configuration are shown in table 17.

Table 17**:** Areal densities of WS configurations

Non-ballistic weight	0.069 g/cm2
Rear wall	0.162 g/cm2
Front wall	0.068 g/cm2
Total	0.299 g/cm2

D. Operational Safety and Performance Metrics

Upon analyzing at the design and specifications of the reactor the depth of the bin is 5 meters deep with a width of 9 meters and length of 5 meters. During the excavation process, 11 trenches of radius 2 meters and length of 30 meters each must be dug out to place the heat dissipation radiation arrays. For the arrays most of the excavated regolith can be placed around the trenches to increase the depth of the trenches and reduce the amount of sunlight entering the trenches. And the remaining amount of regolith obtained from excavating the reactor bin is to be used to create a mound of regolith of 10 meters thick to provide shielding from the reactor. On analyzing the effective shielding provided by each material available in the lunar regolith, a mixture of aluminum and iron can be used as the shielding material within the bin.

To reduce the reliance of the reactor heat dissipation on the radiators a feasibility study into using PCM or Phase Change Materials was done using PCM H535 as the preferred material to be used, this PCM was measured to be used in conjunction to the radiators such that during lunar day when the radiators are not able to work effectively the PCM's would absorb the thermal energy from the working fluid to reduce the stress on the radiators, but due to the high density and weight of the PCM materials along with the low rate of absorption this method is discarded, instead the increase in number of radiator array satisfy the need of heat dissipation during lunar day, without drastically increasing the weight of the heat dissipation systems.

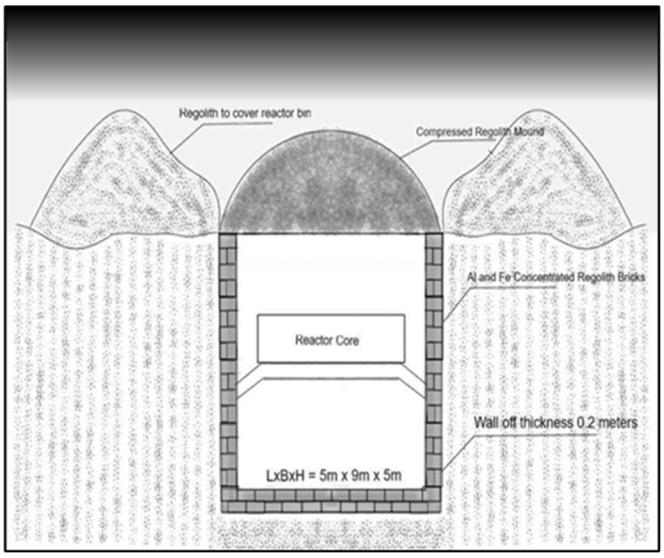

Figure 15. Reactor emplacement design cross-section.

Some of the important safety protocols that are to be considered when operating the moonbase includes the meltdown protocol which when active and determined that the reactor cannot be saved, the legs holding the reactor within the bin will break off plunging the reactor into the bin and the mound of regolith above the bin will break and apply the lunar regolith over the reactor completely submerging the reactor, after this lunar regolith placed on the side of the reactor bin will be introduced over the bin and a covering will be made of where the reactor mound used to exist. Another important aspect for safety includes having 24/7 supervision of the reactor and its components by a nuclear engineer present at the moonbase to ensure swift action.

The use of robots and rovers for the maintenance and operation of the nuclear reactor and its corresponding systems is a potential safety risk as the ability of robots and rovers to perform complex tasks within an acceptable timeframe is not sufficient enough to prevent a nuclear accident. Introducing human beings into the moonbase increases the flexibility of tasks that can be done and also the period of time within which each task can be done. Taking into consideration the different requirements for humans upon the moonbase from table 16, the final FTE for operations of the reactor and moonbase maintenance by humans is 20 FTE. Along with this accounting for the energy needs of each human which includes all corresponding life systems at 15 kW per person is 291 kW for the entire human operations on the base.

FTE Table				
	Tasks	Hrs.	FTE's	Energy Req (kW)
Processing	Maintenance	10	0.25	3.75
Transmutation	Maintenance	10	0.25	3.75
	Radiation Expert	56	1.4	21
Reactor	Maintenance	27	0.675	10.125
	Supervisor	168	4.2	63
C.O and Base Op		168	4.2	63
Commander		168	4.2	63
Medical		168	4.2	63
Total		775	19.375	290.625

Table 18. Lunar base Full Time Equivalents (FTE).

CONCLUSIONS

Presented here for the first time is a study of the first lunar nuclear reactor, built in one year's time, in which the only radioactive material is drawn from, and process on, the Earth's Moon. This first-generation moon base power station produces 2000 kW of baseload power with ample waste heat for useful purposes. Operational lifetime is estimated at just over six years. At end-of-life, the control rods are fully inserted and the reactor is buried. The site must be marked so that the warning signs are still understandable 100 years from now, after which time the reactor will present less of a radiation threat than the deep space background. When started in this way, a blossoming ISRU economic sphere will be created, as well as a base of operations for scientific inquiry and investigations. Most important, with this Gen One reactor operational, improved processing methods can be used to make greater refinements in the transmutation of lunar thorium to U-233, so that second generation nuclear reactors using nuclear fuel from lunar regolith can be of considerably higher performance and longevity. The total system mass, with reactor, radiators, turbomachinery, cables, plus the beneficiation equipment to produce the uranium, is 53.4 MT.

ACKNOWLEDGEMENTS

The authors thank Dr. James "Jim" Willit of Argonne National Labs for helpful comments. The authors are also grateful for personal conversations with Dr. Eric Christiansen of NASA JSC.

REFERENCES

1 Kerslake, Thomas W. "Lunar Surface-to-Surface Power Transfer." AIP Conference Proceedings, 2008, doi:10.1063/1.2845004.

2 Tournier, J. P., and El-Genk, M. S, "Transport Properties of He-N_2 Binary Gas Mixtures for CBC Space Applications. United States": N. p., 2008. Web. doi:10.1063/1.2845025.

3 Lemmon, E.W., McLinden, M.O, and Friend, D.G., "Thermophysical Properties of Fluid Systems" in NIST Chemistry WebBook, NIST Standard Reference

Database Number 69, Eds. P.J. Linstrom and W.G. Mallard, https://doi.org/10.18434/T4D303, (retrieved June 8, 2020).
4 La Fleur, J. K., "Description of an Operating Closed-Cycle Helium Gas Turbine," ASME Paper No. 63-AHGT-74.
5 Christiansen, E. Personal communication with E. Christiansen of NASA JSC, August 12, 2020.
6 Cherniaev, A. and Telichev, I., "Weight-Efficiency of Conventional Shielding Systems in Protecting Unmanned Spacecraft from Orbital Debris," 2016. Journal of Spacecraft and Rockets. 54. 1-15. 10.2514/1.A33596.
7 Juhasz, A., "Multi-Megawatt Gas Turbine Power Systems for Lunar Colonies," 2006, 10.2514/6.2006-4117.
8 Lawrence, D., Feldman, W., Barraclough, Bruce, Binder, A.B., Elphic, R., Maurice, S., Miller, M. and Prettyman, T., "Thorium abundances on the lunar surface. Journal of Geophysical Research." 2000. 105331. 307-20. 10.1029/1999JE001177.:
9 Cedarapids Static Jaw Crushers | Terex MPS". *Terex MPS*, 2020
10 Crushers - All Crusher Types for Your Reduction Needs - Metso". *Metso*, 2020
11 Jaw Crushers | Telsmith". *Telsmith*, 2020
12 Jaw Crushers, Stationary Jaw Crusher Series — Sandvik Mining and Rock Technology". *Rocktechnology.Sandvik*, 2020
13 Rock Crushing Theory and Formula Using Kick & Rittinger's Law". *Mineral Processing & Metallurgy*, 2020
14 Berk, Zeki. *Food Process Engineering and Technology*. Academic, 2009.
15 Surampudi, Subbarao. "Overview of The Space Power Conversion and Energy Storage Technologies". *Lpi.Usra.Edu*, 2011
16 Zolensky, M., Bland, Phil, Brown, Peter, Halliday, I.Flux of Extraterrestrial Materials. Meteorites and the Early Solar System II, accessed 7 Sep 2020: 2006,https://www.researchgate.net/publication/241238899_Flux_of_Extraterrestrial_Materials.
17 Kaczmarzyk, Marcin & Gawronski, Marcin & Piatkowski, Grzegorz. Global database of direct solar radiation at the Moon's surface for lunar engineering purposes. E3S Web of Conferences. 49. 00053. 10.1051/e3sconf/20184900053, 2008.
18 Mason, L., Shaltens, R., Dolce, J. and Cataldo, R., "Status of Brayton cycle power conversion development at NASA GRC." 2002: 608. 10.1063/1.1449813.
19 Olumayegun, O., Wang, M. and Kelsall, G., "Closed-cycle gas turbine for power generation: A state-of-the-art review" 2016. Fuel. 180. 694-717. 10.1016/j.fuel.2016.04.074.
20 Dasarathi Das, and S. R. Bharadwaj. Thoria-Based Nuclear Fuels: Thermophysical and Thermodynamic Properties, Fabrication, Reprocessing, and Waste Management. Springer, 2013
21 Malik, A., Zheng, Q., Qureshi, S., and Zaidi, A.A., "Effect of helium xenon as working fluid on the compressor of power conversion unit of closed Brayton cycle HTGR power plant".2020 International Journal of Hydrogen Energy. 45. 10119-10129. 10.1016/j.ijhydene.2020.01.220.
22 Flessas, S., "The Vital Role of Specialized Compressors In Helium Recovery | Compressed Air Best Practices." 2020.https://www.airbestpractices.com/industries/medical/vital-role-specialized-compressors-helium- recovery> [Accessed August 2020].
23 Juhasz, A., "Space & Terrestrial Power System Integration Optimization Code BRMAPS for Gas Turbine Space Power Plants with Nuclear Reactor Heat Sources," 2007: CSU Lecture on Thorium
24 Kofskey, M. G., and Glassman, A. J. "Turbomachinery Characteristics of Brayton-Cycle Space-Power-Generation Systems." Proceedings of the ASME 1964 Gas Turbine Conference and Products Show. ASME 1964 Gas Turbine Conference and Products Show. Houston, Texas, USA. March 1–5, 1964. V001T01A023. ASME. https://doi.org/10.1115/64-GTP-23
25 Linares, J., Arenas, E., Cantizano, A., Porras, J., Moratilla, B., Carmona, M., Batet, L., "Sizing of a recuperative supercritical CO_2 Brayton cycle as power conversion system for DEMO fusion reactor based on Dual Coolant Lithium Lead blanket." Fusion Engineering and Design, 2018. 134. 10.1016/j.fusengdes.2018.06.026.
26 Christopher G. M., "Temperature and Power Specific Mass Scaling for Commercial Closed-Cycle Brayton Systems in Space Surface Power and Nuclear Electric Propulsion Applications," 2020 Nuclear Technology, 206:8, 1224-1239, DOI: 10.1080/00295450.2020.1738173
27 Juhasz, A. J., "Analysis and Numerical Optimization of Gas Turbine Space Power Systems with Nuclear Fission Reactor Heat Sources," PhD Dissertation, Cleveland State University (2005).
28 Vericor Power Systems, www.vericor.com: accessed August 2020
29 Solar Turbines, accessed August 2020, www.solarturbines.com/en_US/index.html:
30 J.P. Sauer & Sohn Maschinenbau GmbH, accessed August 2020, https://www.sauercompressors.com/ :
31 THE SWITCH, https://theswitch.com/: accessed August 2020
32 Mecc Alte, https://www.meccalte.com/: accessed August 2020
32 ABB, https://global.abb/group/en: accessed August 2020
33 Earle, R.L., Unit Operations in Food Processing, 2nd Ed., Pergamon, 1983, Pergamon Press: ISBN 0-08-025537-X
34. Yacout, Abdellatif., "Nuclear Fuel," Argonne National Laboratory, https://www.ne.anl.gov/pdfs/nuclear/nuclear_fuel_yacout.pdf
35.Afifi, Y.K., El-Hakim, E., Abdelrazek, I.D., "Qualification of sintered uo2 pellets," International Atomic Energy Agency. Cairo, Egypt.